

Geology, geochronology, and geochemistry of basaltic flows of the Cat Hills, Cat Mesa, Wind Mesa, Cerro Verde, and Mesita Negra, central New Mexico

Florian Maldonado, James R. Budahn, Lisa Peters, and Daniel M. Unruh

Abstract: The geochronology, geochemistry, and isotopic compositions of basaltic flows erupted from the Cat Hills, Cat Mesa, Wind Mesa, Cerro Verde, and Mesita Negra volcanic centres in central New Mexico indicate that each of these lavas had unique origins and that the predominant mantle involved in their production was an ocean-island basalt type. The basalts from Cat Hills (0.11 Ma) and Cat Mesa (3.0 Ma) are similar in major and trace element composition, but differences in MgO contents and Pb isotopic values are attributed to a small involvement of a lower crustal component in the genesis of the Cat Mesa rocks. The Cerro Verde rock is comparable in age (0.32 Ma) to the Cat Hills lavas, but it is more radiogenic in Sr and Nd, has higher MgO contents, and has a lower La/Yb ratio. This composition is explained by the melting of an enriched mantle source, but the involvement of another crustal component cannot be disregarded. The Wind Mesa rock is characterized by similar age (4.01 Ma) and MgO contents, but it has enriched rare-earth element contents compared with the Cat Mesa samples. These are attributed to a difference in the degree of partial melting of the Cat Mesa source. The Mesita Negra rock (8.11 Ma) has distinctive geochemical and isotopic compositions that suggest a different enriched mantle and that large amounts of a crustal component were involved in generating this magma. These data imply a temporal shift in magma source regions and crustal involvement, and have been previously proposed for Rio Grande rift lavas.

Résumé : Les compositions géochronologiques, géochimiques et isotopiques des coulées basaltiques qui ont fait éruption des centres volcaniques de Cat Hill, de Cat Mesa, de Wind Mesa, de Cerro Verde et de Mesita Negra dans le centre du Nouveau-Mexique indiquent que chacune de ces laves a une origine unique et que le manteau principal qui les a produites est du type basalte océanique insulaire (OIB). Les basaltes provenant de Cat Hills (0,11 Ma) et de Cat Mesa (3,0 Ma) ont des compositions en éléments majeurs et en éléments traces similaires; cependant les différents teneurs en MgO et les valeurs isotopiques Pb sont attribuées à une faible implication d'une composante de la croûte inférieure dans la genèse des roches de Cat Mesa. Les roches de Cerro Verde ont un âge (0,32 Ma) comparable aux laves de Cat Hills mais elles ont des teneurs radiogéniques Sr et Nd plus élevées ainsi qu'un contenu en MgO plus élevé et un rapport La/Yb plus faible. Cette composition est expliquée par la fusion d'une source mantellique enrichie mais l'implication d'une autre composante de la croûte ne peut être écartée. Les roches de Wind Mesa (4,01 Ma) sont caractérisées par un âge et une teneur en MgO similaires mais aussi par un enrichissement de la teneur en éléments de terres rares comparativement aux échantillons de Cat Mesa. Ces caractéristiques sont attribuées à une différence dans le degré de fusion partielle de la source de Cat Mesa. Les roches de Mesita Negra (8,11 Ma) ont des compositions géochimiques et isotopiques distinctives qui suggèrent un manteau enrichi différent et que de grandes quantités d'une composante de la croûte soient impliquées dans la génération de ce magma. Ces données indiquent un changement des régions sources du magma avec le temps ainsi que l'implication de la croûte, tel que déjà été proposé antérieurement pour les laves du rift du Rio Grande.

[Traduit par la Rédaction]

Introduction

The geologic setting, geochronology, and geochemistry are discussed for the following volcanic fields: Cat Hills, Cat

Mesa, Wind Mesa, Cerro Verde, and Mesita Negra. Ages for samples were determined at the New Mexico Geochronological Research Laboratory in Socorro, New Mexico, and geochemical analyses were conducted at the laboratories of the US Geo-

Received 22 April 2005. Accepted 16 February 2006. Published on the NRC Research Press Web site at <http://cjcs.nrc.ca> on 25 October 2006.

Paper handled by Associate Editor J.D. Greenough.

F. Maldonado.¹ US Geological Survey, P.O. Box 25046, MS 980, Denver, CO 80225, USA.

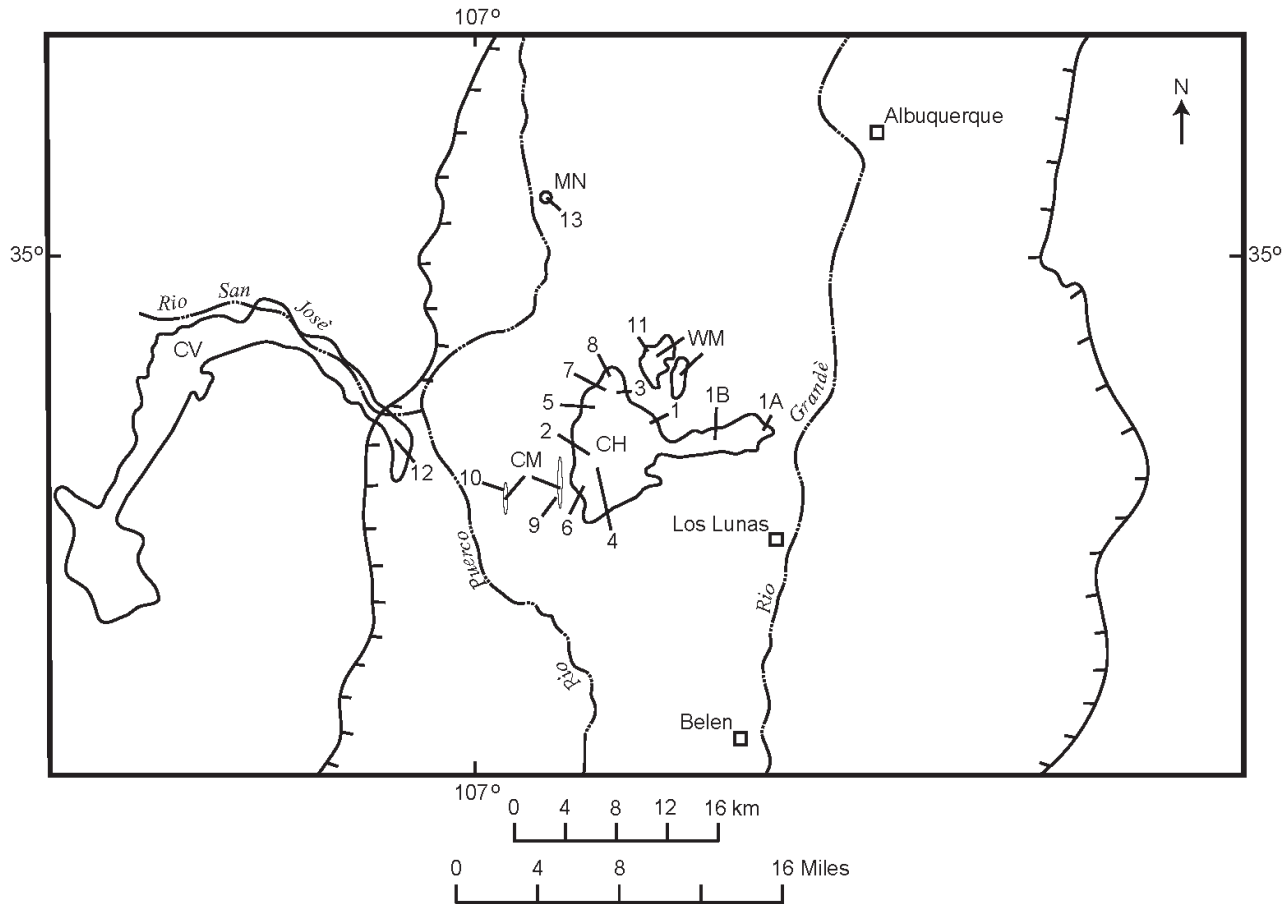
J.R. Budahn. US Geological Survey, P.O. Box 25046, MS 973, Denver, CO 80225, USA.

L. Peters. New Mexico Bureau of Geology and Mineral Resources, Socorro, NM 87801, USA.

D.M. Unruh. US Geological Survey, P.O. Box 25046, MS 963, Denver, CO 80225, USA.

¹Corresponding author (e-mail: fmaldona@usgs.gov).

Fig. 1. Location map for Cat Hills, Cat Mesa, Wind Mesa, Cerro Verde, and Mesita Negra volcanic fields. Numbers indicate rock sample locations. Hachured lines indicate Rio Grande rift boundary. Modified from Kelley and Kudo (1978). CH, Cat Hills; CM, Cat Mesa; WM, Wind Mesa; CV, Cerro Verde; MN, Mesita Negra.



logical Survey (USGS) in Denver, Colorado. The study area is located west of the Rio Grande and along the Rio Puerco and Rio San José, west and southwest of Albuquerque, New Mexico (Fig. 1). The geology for parts of the study area was mapped by Kelley and Kudo (1978) and more recently by Maldonado and Atencio (1998a, 1998b) and Maldonado (2003). The geology of the area has been summarized by Maldonado et al. (1999) and the reader is referred to that report for more geologic details.

Previous studies of continental rift basalts (CRB) have shown that there is a wide range of compositions in the erupted lavas, suggesting that there are multiple source components involved in their generation. For example, assimilation of lower crust and melting of two isotopically distinct mantle sources are suggested to account for the composition of Oligocene mafic rocks (26 Ma) from the San Luis Hills volcanic area (Johnson and Thompson 1991) of the Rio Grande rift. A study of magmatism along the Rio Grande rift in southern New Mexico (McMillan et al. 2000) suggests that the compositions of these igneous rocks with respect to age record a shift in magma source regions from lithosphere to asthenosphere and from upper crust to lower crust, with the most recent lavas exhibiting little crustal involvement. Oligocene basalts (>26 Ma) are interpreted as partial melts of a hydrated lithosphere, whereas the Miocene

lavas (<10 Ma) have compositions similar to ocean-island basalts (OIB). A similar conclusion was reached in a more recent investigation of extension-related magmatism that occurred during the formation of the Sea of Japan (Okamura et al. 2005), although the asthenospheric component of the mid-Miocene–Pliocene lavas (14–5 Ma) in this study is thought to consist of a mid-oceanic ridge basalt (MORB) type source. Some of the mid-Miocene Japanese basalts were generated from subduction-modified lithospheric mantle. Thus, it is generally accepted that the wide range of rift-related basalt compositions can be explained by heterogeneities of the mantle source regions.

In this paper, we present age, major element, trace element, and isotopic data that indicate most of the igneous rocks from the Cat Hills volcanic field were predominantly derived from the melting of an OIB-type source, although a MORB contribution can not be completely discounted. Only two samples collected from these fields appear to have any significant crustal involvement.

Geologic setting

The flows of the Cat Hills, Cat Mesa, Wind Mesa, Mesita Negra, and Cerro Verde were erupted during or after deposition of the Santa Fe Group sediments. The Santa Fe Group sedi-

Fig. 2. (a) View looking east towards aligned chain of Cat Hills cinder cones. Blackbird cone (BC) at northern end of chain and Floripa cone (FC) at southern end. (b) View looking south of Floripa cone, highest cone in the Cat Hills chain. (c) Photograph of basalt of Cat Mesa interbedded with the Ceja Formation of the Santa Fe Group. Tcm, Cat Mesa basalt. (d) Photograph of Wind Mesa volcanic field.

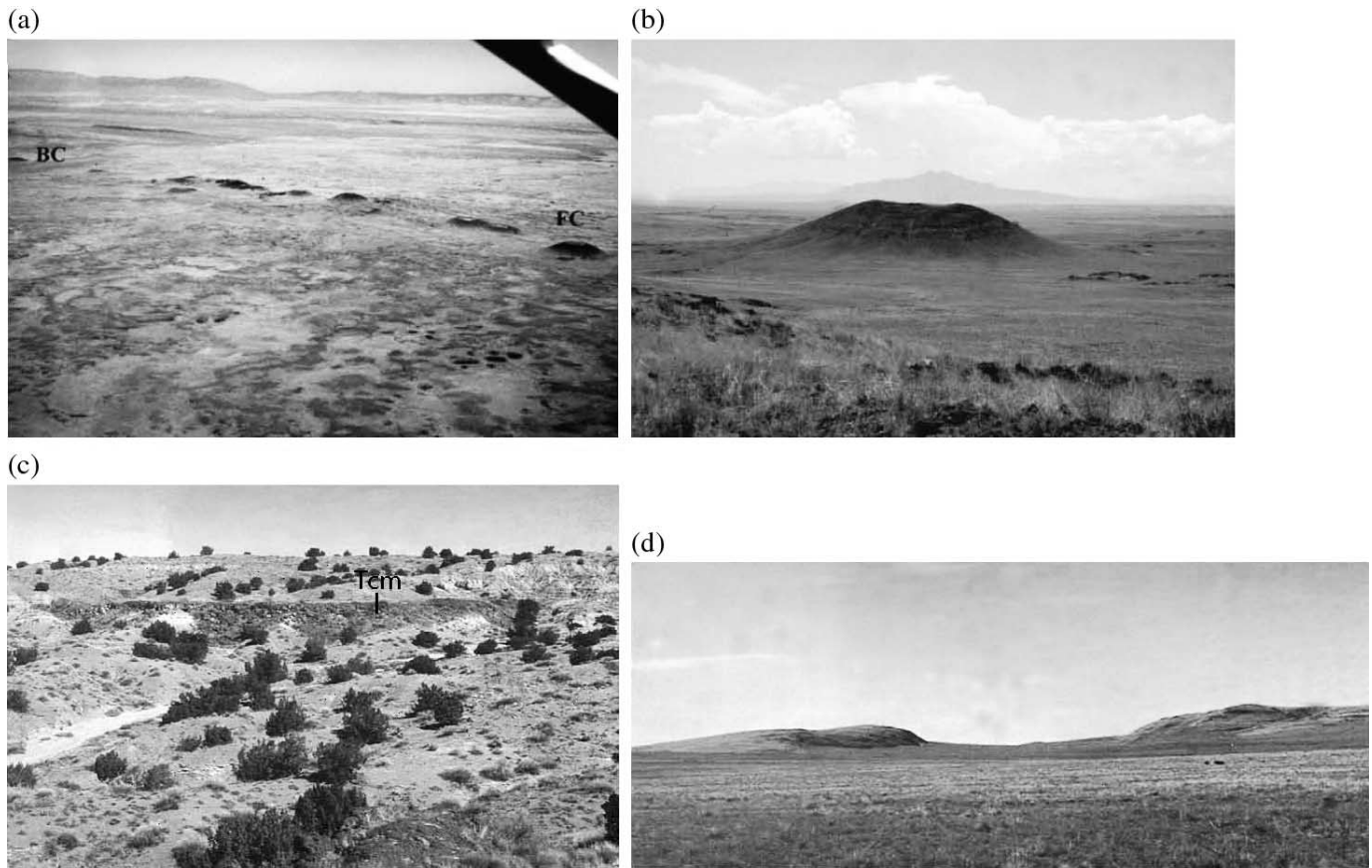


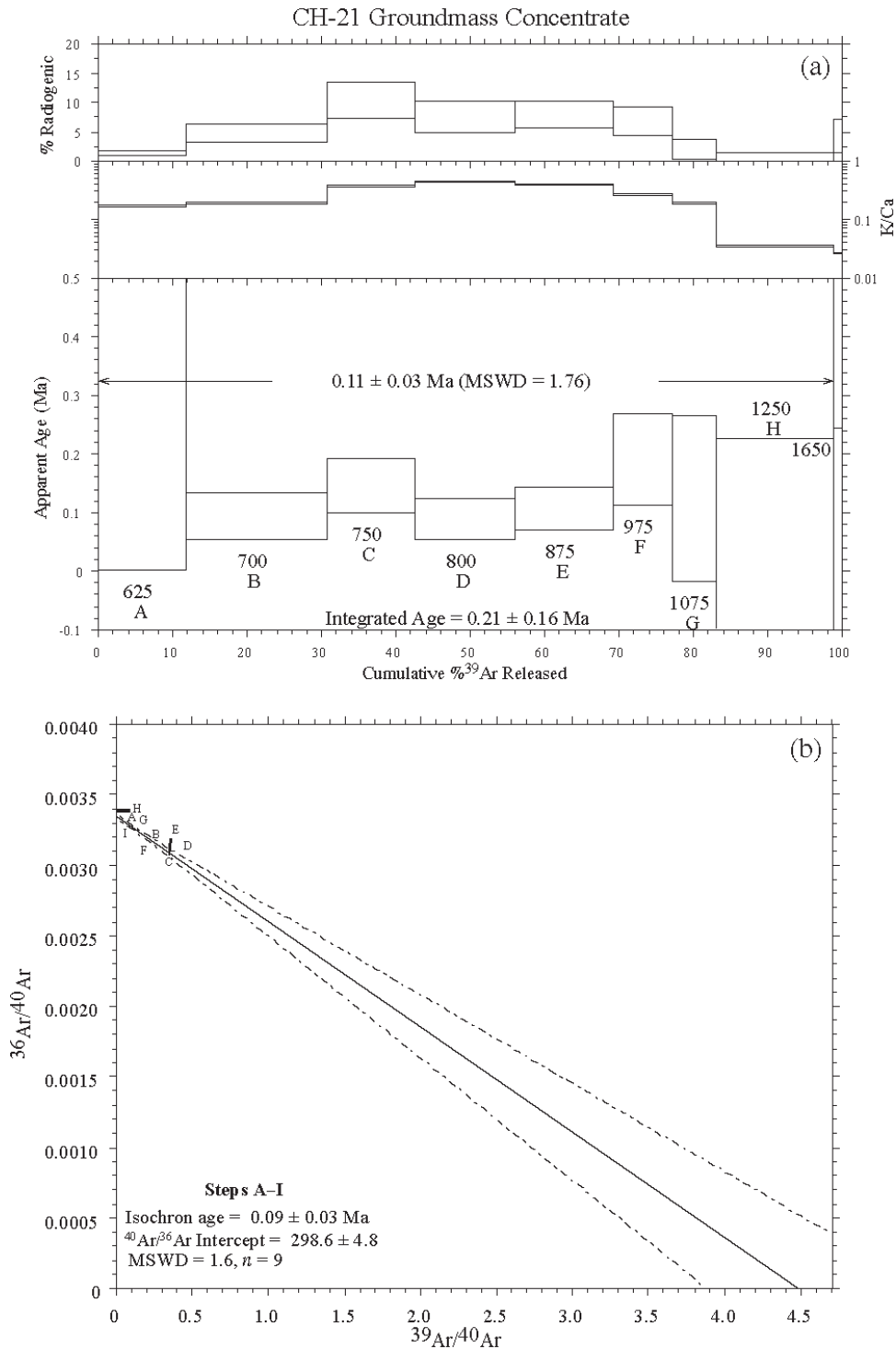
Table 1. Sample numbers and age determinations of the Cat Hills, Cat Mesa, Wind Mesa, Cerro Verde, and Mesita Negra lava flows.

Lab No.	Sample location number (Fig. 1)	Longitude, Latitude	Flow units from Maldonado and Attencio (1998a, 1998b)	Flow units from Kelley and Kudo (1978)	Age
CH-21	1	106°50'22", 34°53'28"	Qch1	Qb1	98±0.02 ka (⁴⁰ Ar/ ³⁹ Ar) ^a
	1A	106°44'52", 34°52'36"	Qch1	Qb1	110±0.30 ka (⁴⁰ Ar/ ³⁹ Ar) ^a
	1B	106°47'39", 34°51'44"	Qch1	Qb1	140±0.038 ka (K/Ar) ^b
CH-07	2	106°53'33", 34°51'00"	Qch2	Qb1a	
CH-02	3	106°50'50", 34°54'05"	Qch3	Qb2	
CH-08	4	106°20'11", 34°50'28"	Qch4	Qb2a	
CH-03	5	106°51'55", 34°53'42"	Qch5	Qb3	
CH-05	6	106°53'54", 34°50'49"	Qch6	Qb3a	
CH-06A	7	106°51'59", 34°53'58"	Qch7	Qb4	
CH-09A	8	106°52'18", 34°55'16"	Cat Hills dike in cone of Blackbird		
CM-04	9	106°55'20", 34°50'31"	Tcm-Cat Mesa flow	Tbcm	
CM-01A	10	106°57'14", 34°51'15"	Tcm-Cat Mesa flow	Tbcm	3.00±0.10 Ma (⁴⁰ Ar/ ³⁹ Ar) ^a
WM-01A	11	106°50'40", 34°56'18"	Twml-Wind Mesa flow 1	Tbf	4.01±0.16 Ma (⁴⁰ Ar/ ³⁹ Ar) ^a
CH-10	12	107°2'48", 34°50'37"	Cerro Verde flow		320 Ka ^c
CH-11	13	106°55'51", 35°2'30"	Mesita Negra flow		8.11±0.05 Ma (⁴⁰ Ar/ ³⁹ Ar) ^a

^aSource: Maldonado et al. 1999.

^bSource: Kelley and Kudo 1978.

^cSource: Leavy et al. 1987.

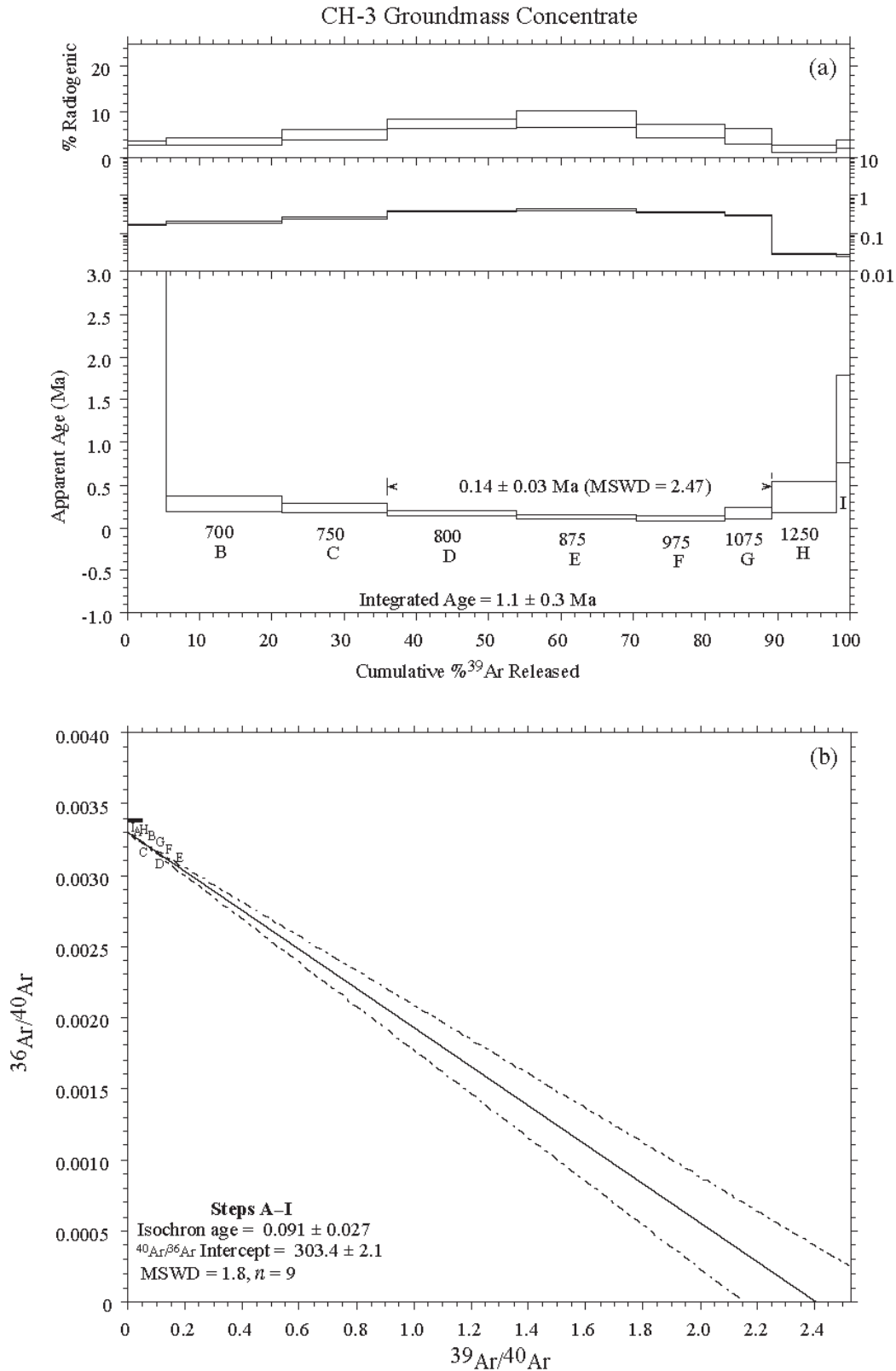
Fig. 3. Age spectrum (a) and isochron (b) for sample CH-21 (Cat Hills) groundmass concentrate. All error quoted as 2σ .

ments are Neogene fluvial sediments that were deposited in basins formed along the Rio Grande rift. Most of the volcanic rocks were erupted within the Rio Grande rift, except for the Cerro Verde, which erupted adjacent to the rift in the Colorado Plateau area.

The Cat Hills volcanic field is located about 29 km southwest of Albuquerque (Fig. 1) and is composed of seven flows and 21 cinder cones (Figs. 2a, 2b) (Kelley and Kudo

1978; Maldonado and Atencio 1998a, 1998b; Maldonado et al. 1999; and Maldonado 2003). Flows are dark gray to grayish black, vesicular, occasionally porphyritic, basaltic, (Kelley and Kudo 1978), and contain phenocrysts of plagioclase and olivine with some clinopyroxene and opaque minerals. The oldest flow has been dated at 110 ± 0.03 and 98 ± 0.02 ka using the $^{40}\text{Ar}/^{39}\text{Ar}$ method (Maldonado et al. 1999) and 140 ± 0.038 ka using the K/Ar method (Kudo et al.

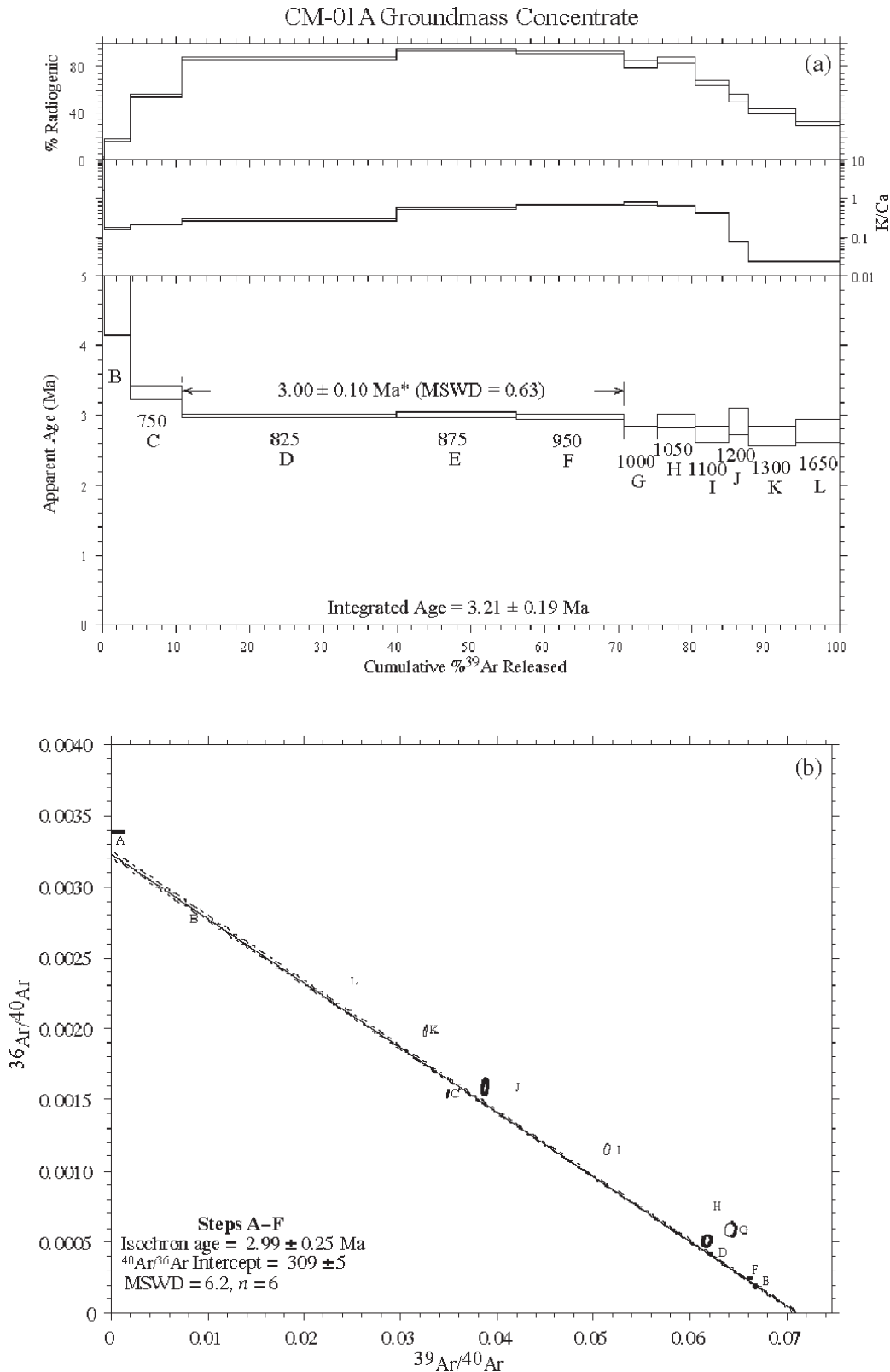
Fig. 4. Age spectrum (a) and isochron (b) for sample CH-3 (Cat Hills) groundmass concentrate. All errors quoted at 2σ .



1977). These flows overlie calcic soils of Stage II–III carbonate morphology (Maldonado et al. 1999) that in turn overlie the Ceja Formation of the Santa Fe Group.

The Cat Mesa flow is located ~35 km southwest of Albuquerque (Fig. 1). The flow (Fig. 2c) is composed of dark gray to grayish black porphyritic basaltic flow with a micro-

Fig. 5. Age spectrum (a) and isochron (b) for sample CM-01A (Cat Mesa) groundmass concentrate. Steps G–L not included in isochron. All errors quoted at 2σ .



granular groundmass that contains plagioclase, olivine, clinopyroxene, and Fe–Ti oxides. Phenocrysts (1–5 mm) make up as much as 87% of rock and include plagioclase, clino-

pyroxene, and olivine in 6:3:1 proportions, as well as Fe–Ti oxides. A single flow dated at 3.00 ± 0.10 Ma by $^{40}\text{Ar}/^{39}\text{Ar}$ method (Maldonado et al. 1999) lies on top of the lower

Fig. 6. Age spectrum (a) and isochron plot (b) for sample WM-01A (Wind Mesa) groundmass concentrate. All errors quoted at 2σ .

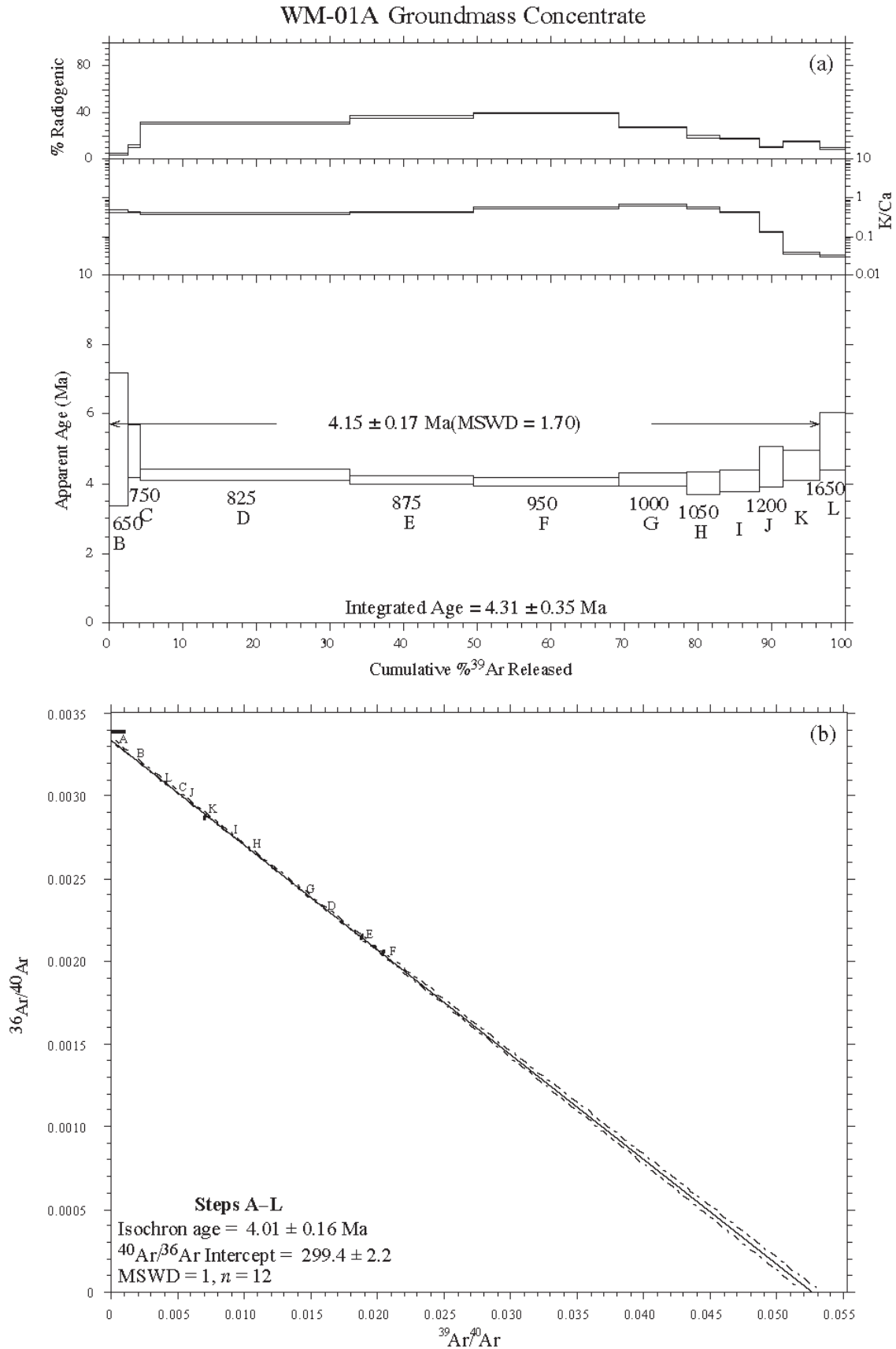
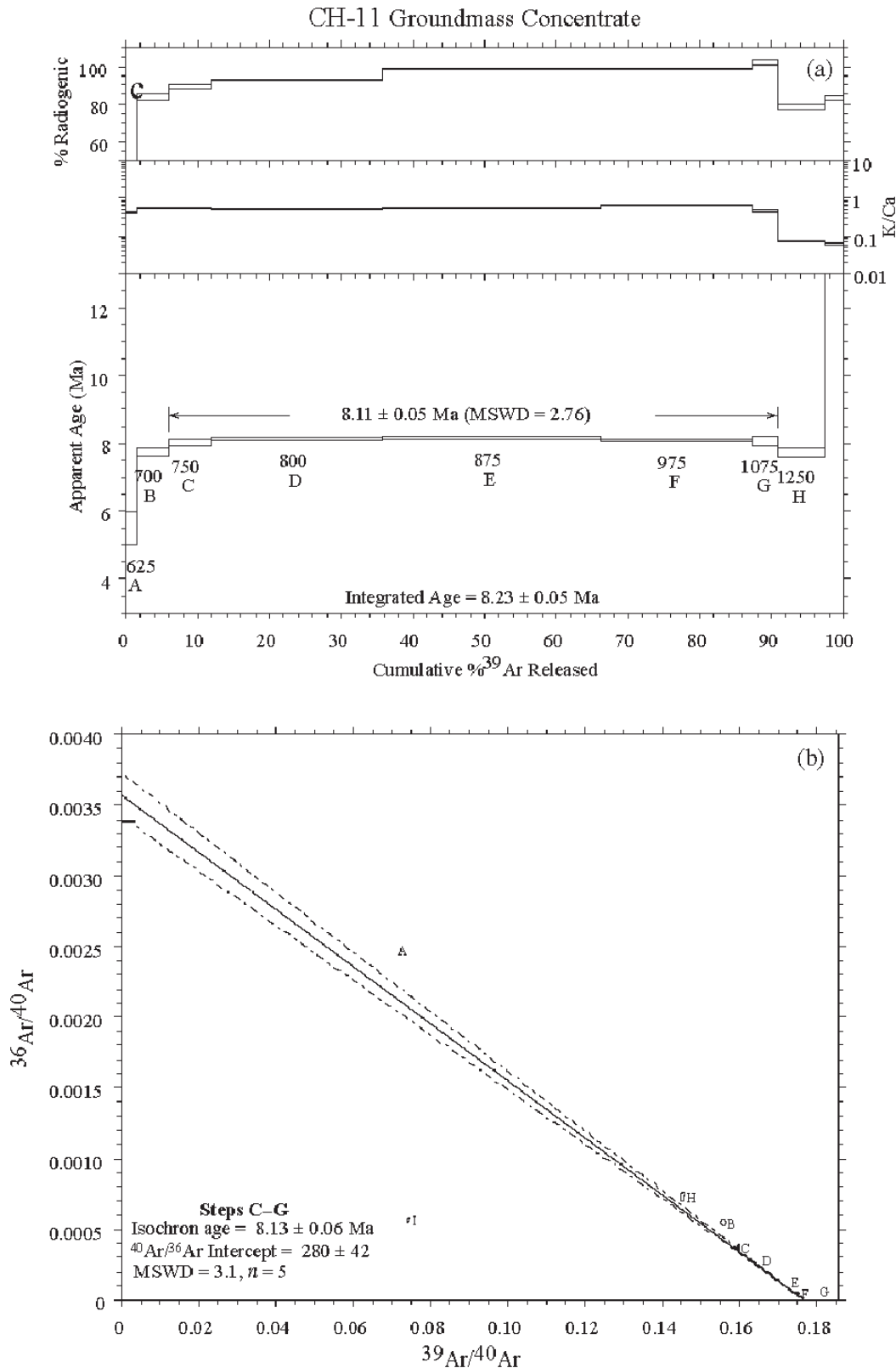


Fig. 7. Age spectrum (a) and isochron (b) for sample CH-11 (Cat Hills) groundmass concentrate. Steps A, B, H, and I not included in isochron. All errors quoted at 2σ .



sand and gravel unit of the Ceja Formation of the Santa Fe Group, and it is covered by the middle silt, sand, and clay unit of the Ceja Formation (Maldonado 2003).

The Wind Mesa volcanic field (Fig. 2d) is located about 23 km southwest of Albuquerque (Fig. 1) and includes three flow units that are medium dark gray to dark gray, multiple,

Table 2. Chemical composition and modified CIPW norms of Cat Hills, Cat Mesa, Wind Mesa, Cerro Verde, and Mesita Negra flows from this study.

	Wind Mesa	Cat Hills								Cat Mesa		Cerro Verde	Mesita Negra	Columbia River basalt	BHVO-1	
	WM-01A (Twm1)	CH-21 (Qch1)	CH-7 (Qch2)	CH-2 (Qch3)	CH-8 (Qch4)	CH-3 (Qch5)	CH-5 (Qch6)	CH-06A (Qch7)	CH-9A (Cat Hills dike)	CM-04 (Tcm)	CM-01A (Tcm)	CH-10 (Cerro Verde flow)	CH-11 (Mesita Negra flow)	Basaltic volcanism study project (1981)	WD-XRF USGS	Velasco Tapia et al. 2001
SiO ₂ ^a	51.88	48.61	48.47	48.49	47.08	49.45	49.46	49.34	49.26	49.40	49.70	50.53	49.62	48.35	50.30	50.00
TiO ₂ ^a	1.52	1.80	1.78	1.80	1.75	1.94	1.80	1.97	1.82	1.75	1.81	1.56	1.60	1.57	2.78	2.84
Al ₂ O ₃ ^a	16.36	15.89	15.52	15.49	15.38	16.44	15.80	16.22	15.76	16.77	17.02	14.98	16.90	15.49	13.82	13.80
FeTO ₃ ^a	9.09	12.39	12.04	12.21	12.24	11.26	11.78	11.19	12.05	11.77	11.68	12.23	8.18	12.20	12.34	12.34
MnO ^a	0.14	0.18	0.17	0.18	0.17	0.16	0.17	0.16	0.17	0.16	0.16	0.17	0.10	0.17	0.17	0.17
MgO ^a	5.77	7.98	7.66	8.03	8.18	6.44	6.89	6.36	7.08	5.68	5.23	8.26	2.47	7.03	7.28	7.22
CaO ^a	8.15	9.21	9.32	9.12	9.23	9.25	9.34	9.33	9.12	9.57	9.46	8.50	10.14	9.92	11.49	11.41
Na ₂ O ^a	3.78	3.23	3.09	3.14	3.03	3.36	3.14	3.38	3.14	3.41	3.49	2.85	4.00	2.76	2.23	2.26
K ₂ O ^a	1.60	1.00	0.97	1.06	0.87	1.20	1.02	1.19	0.93	0.98	1.00	0.76	1.98	0.51	0.53	0.51
LOI ^a	0.54	-0.60	0.34	-0.16	1.53	0.12	-0.05	-0.12	0.11	0.29	0.27	0.04	3.84	1.52	0.15	0.16
P ₂ O ₅ ^a	0.61	0.40	0.40	0.42	0.35	0.47	0.42	0.46	0.37	0.31	0.32	0.21	0.49	0.24	0.30	0.28
Total	98.90	100.69	99.42	99.94	98.28	99.97	99.82	99.60	99.70	99.80	99.87	100.05	95.48	99.76	101.24	100.82
Or ^b	9.627	5.933	5.827	6.335	5.289	7.162	6.099	7.127	5.567	5.862	5.975	4.538	12.333	3.102		
Ab ^b	32.569	27.433	26.57	26.866	26.366	28.71	26.891	28.99	26.925	29.201	29.87	24.353	30.742	24.023		
An ^b	23.367	25.997	26.031	25.317	26.524	26.495	26.314	25.923	26.512	27.894	28.135	26.096	23.519	29.188		
Ne ^b	—	—	—	—	—	—	—	—	—	—	—	—	2.676	—		
Di ^b	11.139	14.072	14.949	14.4	14.853	13.705	14.57	14.692	13.822	14.916	14.208	12.327	21.636	16.254		
Hy ^b	12.978	1.099	4.803	2.865	0.695	4.52	9.058	3.872	9.699	4.03	5.227	21.779	-	13.742		
Ol ^b	2.728	18.357	14.737	17.046	19.235	12.071	9.988	12.014	10.401	11.371	9.746	4.69	1.697	7.276		
Mt ^b	3.214	2.749	2.705	2.73	2.784	2.514	2.636	2.508	2.7	2.634	2.612	2.731	2.994	2.775		
Il ^b	2.94	3.43	3.436	3.457	3.419	3.721	3.459	3.793	3.502	3.364	3.476	2.993	3.204	3.067		
Ap ^b	1.439	0.929	0.941	0.985	0.834	1.1	0.985	1.08	0.869	0.728	0.751	0.491	1.196	0.572		
Mg#	62.312	60.087	59.794	60.588	60.97	57.208	57.756	57.055	57.868	53.01	51.139	61.221	44.028	57.391		

Note: Map symbols (Twm1, Qch1, etc.) from Maldonado and Atencio (1998a, 1998b). LOI, loss on ignition.

^aValues in percent.

^bValues are CIPW norms in wt.%.

Table 3. Trace elements of the Wind Mesa, Cat Hills, Cat Mesa, Cerro Verde, and Mesita Negra lava flows.

Volcanic centre:	Wind Mesa	Cat Hills								Cat Mesa		Cerro Verde	Mesita Negra		
Element ^a	WM-01A (Twm1)	CH-21 (Qch1)	CH-7 (Qch2)	CH-2 (Qch3)	CH-8 (Qch4)	CH-3 (Qch5)	CH-5 (Qch6)	CH-6A (Qch7)	CH-9A (Cat Hills dike)	CM-4 (Tcm)	CM-1 (Tcm)	CH-10 (Cerro Verde flow)	LMN (Mesita Negra flow)	BHVO-1 (INAA-USGS)	BHVO-1 (Velasco- Tapia et al. 2001)
FeO	8.25	11.42	10.76	10.51	10.9	9.98	10.54	10.15	10.76	10.42	10.36	10.9	7.33	11.00	11.11
CaO	8.3	8.83	9.02	9.21	9.78	9.01	9.37	8.97	8.62	9.79	9.68	8.09	10.34	11.50	11.41
Na ₂ O	3.8	3.29	3.09	2.99	3.05	3.34	3.17	3.41	3.17	3.38	3.48	2.83	4.06	2.20	2.26
K ₂ O	1.47	1	0.95	1.07	0.84	1.11	0.89	1.23	0.93	1.03	0.99	0.77	1.89	0.57	0.508
Rb	22.3	9.91	11	14.1	3.69	7.35	15.2	11.9	11.1	11.6	12.2	18	32.7	11.1	11.4
Sr	1010	486	424	409	439	490	450	481	414	413	448	299	708	418	410
Cs	0.419	0.0939	0.138	0.227	0.036	0.0366	0.208	0.0623	0.165	0.0532	0.0271	1.44	0.172	0.11	
Ba	957	239	945	391	375	285	266	322	230	251	253	196	885	122	140
Th	4.28	1.67	1.59	1.65	1.49	1.85	1.75	1.84	1.65	1.24	1.26	1.59	4.02	1.11	1.08
U	1.38	0.465	0.721	0.697	0.581	0.33	0.741	0.462	0.725	0.237	0.343	0.564	1.62	0.44	0.43
La	40.1	17.3	16.6	16.4	14.6	17.9	16.8	18.9	16.2	12.2	13	11.8	31.5	15.5	15.7
Ce	76.2	35.5	32.5	31.9	28	34.7	32.8	36.9	31.2	24.1	26.2	23.9	58.7	37.4	38.8
Nd	35	18.8	17.8	16.6	15.6	18.5	18.5	19.3	16.4	14.2	14.8	14.2	27.2	24.1	25.1
Sm	7.21	4.65	4.53	4.44	4.05	4.52	4.6	4.85	4.35	3.72	4	3.91	5.8	6.41	6.15
Eu	2.01	1.57	1.44	1.43	1.37	1.56	1.5	1.59	1.5	1.36	1.4	1.23	1.75	2.04	2.06
Gd	5.5	4.8	4.64	4.4	4.5	4.54	4.69	5.03	4.67	3.67	4.2	3.99	5.11	6.18	6.3
Tb	0.746	0.707	0.663	0.654	0.596	0.652	0.696	0.678	0.65	0.577	0.622	0.614	0.709	0.87	0.93
Ho	0.931	0.927	0.858	0.822	0.748	0.807	0.898	0.901	0.848	0.762	0.78	0.782	0.929	1.06	0.97
Yb	2.15	2.08	2.09	1.97	1.87	1.83	2.11	2.07	2.06	1.73	1.79	2.09	2.12	2.08	2.01
Lu	0.306	0.293	0.29	0.289	0.254	0.265	0.299	0.285	0.294	0.252	0.272	0.314	0.31	0.277	0.295
Zr	210	159	158	157	151	142	140	156	138	128	134	151	218	184	171
Hf	4.73	3.31	3.12	2.97	3.21	3.6	3.31	3.68	3.41	2.92	3.04	2.94	4.67	4.08	4.32
Ta	2.37	1.54	1.57	1.55	1.4	1.65	1.58	1.82	1.56	1.15	1.21	0.783	2.5	1.21	1.22
W	0.926	0.5	0.5	0.5	0.891	0.5	0.5	0.636	0.5	0.5	0.5	1.54	1.01	0.62	
Sc	19.4	26	25.1	23.7	24.9	24	25.5	25.4	25.1	24.1	24	24.4	20.1	30.2	31.8
Cr	147	265	256	258	289	193	248	193	244	169	157	258	102	270	286
Co	31.7	48.6	43.4	45.8	44.2	36	39.2	36.8	43.3	40.4	42.1	48.9	22.5	42.9	44.9
Ni	86.1	145	124	130	148	86.3	99.7	75.3	97.2	76.2	65.9	209	69.6	108	123
Zn	93.4	76.6	98.2	85.2	74.7	77	96.5	82.3	96.4	89.7	85.6	82.4	64.5	113	104.2
As	0.97	0.457	0.597	0.799	0.924	0.343	0.746	0.536	0.935	1.89	2.08	0.178	4.3	0.42	0.43
Sb	0.126	0.0776	0.0872	0.144	0.12	0.0482	0.105	0.18	0.0923	0.158	0.25	0.0622	0.0976	0.17	0.159
Au (ppb)	0.104	2.7	3.11	1.43	3.13	0.859	0.114	0.17	0.0533	0.752	2.8	1.18	1.44	1.64	1.5

^aOxides are in percent and trace elements are in ppm unless otherwise noted.

Table 4. Pb, Sr, and Nd isotopic data for Cat Hills, Cat Mesa, Wind Mesa, Cerro Verde, and Mesita Negra lava flows.

Sample	$\frac{^{206}\text{Pb}}{^{204}\text{Pb}}$	±	$\frac{^{207}\text{Pb}}{^{204}\text{Pb}}$	±	$\frac{^{208}\text{Pb}}{^{204}\text{Pb}}$	±	$\frac{^{87}\text{Sr}}{^{86}\text{Sr}}$	±	$\frac{^{143}\text{Nd}}{^{144}\text{Nd}}$	±	ϵ_{Nd}
CH-21 (Qch1)	18.174	0.011	15.502	0.014	37.782	0.046	0.703826	0.000015	0.512832	0.000015	3.82
CH-7 (Qch2)	18.217	0.012	15.511	0.015	37.826	0.047	0.703980	0.000036	0.512870	0.000015	4.56
CH-2 (Qch3)	18.190	0.011	15.511	0.014	37.813	0.046	0.703754	0.000020	0.512917	0.000015	5.48
CH-8 (Qch4)	18.212	0.012	15.516	0.014	37.834	0.046	0.703798	0.000020	0.512861	0.000015	4.39
CH-3 (Qch5)	18.308	0.012	15.510	0.015	37.858	0.047	0.703465	0.000021	0.512872	0.000015	4.60
CH-5 (Qch6)	18.222	0.013	15.508	0.016	37.827	0.048	0.703876	0.000021	0.512884	0.000015	4.84
CH-06A (Qch7)	18.322	0.011	15.512	0.014	37.871	0.046	0.703454	0.000024	0.512928	0.000014	5.70
CH-9A (Cat Hills dike)	18.222	0.012	15.501	0.014	37.805	0.046	0.703508	0.000020	0.512855	0.000012	4.27
CM-04 (Tcm)	17.989	0.017	15.520	0.018	37.632	0.053	0.703482	0.000021	0.512877	0.000013	4.70
CM-01A (Tcm)	17.994	0.014	15.520	0.016	37.629	0.049	0.703727	0.000019	0.512873	0.000012	4.62
CH-10 (Cerro Verde flow)							0.706334	0.000020	0.512613	0.000015	-0.45
CH-11 (Mesita Negra flow)	18.145	0.011	15.506	0.014	37.936	0.046	0.704601	0.000019	0.512704	0.000021	1.33

Note: Map symbols are from Maldonado and Atencio (1998a, 1998b).

Table 5. Chemical composition and modified CIPW norms of Wind Mesa and Cat Hills flows.

	Wind Mesa		Cat Hills	
	Flow 1 (sample 8)	Flow 2 (sample 2)	Flow 3 (sample 3)	Flow 5 (sample 5)
SiO ₂ ^a	52.35	49.66	48.4	49.03
TiO ₂ ^a	1.51	1.65	1.72	1.88
Al ₂ O ₃ ^a	16.88	15.60	16.07	16.30
Fe ₂ O ₃ ^a	2.86	2.43	2.64	2.12
FeO ^a	4.62	8.70	8.69	7.72
MnO ^a	0.14	0.19	0.18	0.15
MgO ^a	5.45	7.55	7.80	5.85
CaO ^a	8.28	8.59	8.95	9.68
Na ₂ O ^a	4.04	3.18	3.98	3.43
K ₂ O ^a	1.73	1.10	0.83	1.30
LOI ^a	0.89	0.83	0.46	1.52
P ₂ O ₅ ^a	0.69	0.52	0.40	0.45
Total	99.43	100.00	100.11	99.43
Ap ^b	1.44	1.10	0.83	0.96
Il ^b	2.10	2.32	2.39	2.68
Or ^b	10.21	6.56	4.89	7.85
Ab ^b	36.25	28.81	30.10	31.48
Ne ^b	—	—	3.30	—
Mt ^b	2.99	2.56	2.75	2.27
Hm ^b	—	—	—	—
An ^b	22.82	25.28	23.46	25.82
C ^b	—	—	—	—
Q ^b	0.38	—	—	—
Di ^b	10.99	11.43	14.55	16.22
Hy ^b	12.81	12.24	—	0.85
Ol ^b	—	9.70	17.73	11.87

Note: Source: Kelley and Kudo (1978); LOI, loss on ignition.

^aValues are in percent.

^bValues are CIPW norms in wt.%.

dense to vesicular, and basaltic and basaltic andesite (Kelley and Kudo 1978). The flows contain mostly olivine phenocrysts with some plagioclase, clinopyroxene (~2 mm in length),

and opaque mineral(s) (magnetite?). The oldest exposed flow unit is dated at 4.01 ± 0.16 Ma. (Maldonado et al. 1999) using the ⁴⁰Ar/³⁹Ar method. The volcanic field is exhumed, but flows were probably interlayered with fluvial beds of the Ceja Formation of the Santa Fe Group (Kelley and Kudo 1978; Maldonado and Atencio 1998a). The volcanic field locally includes very dusky red to dark reddish brown basaltic scoria near the vent area.

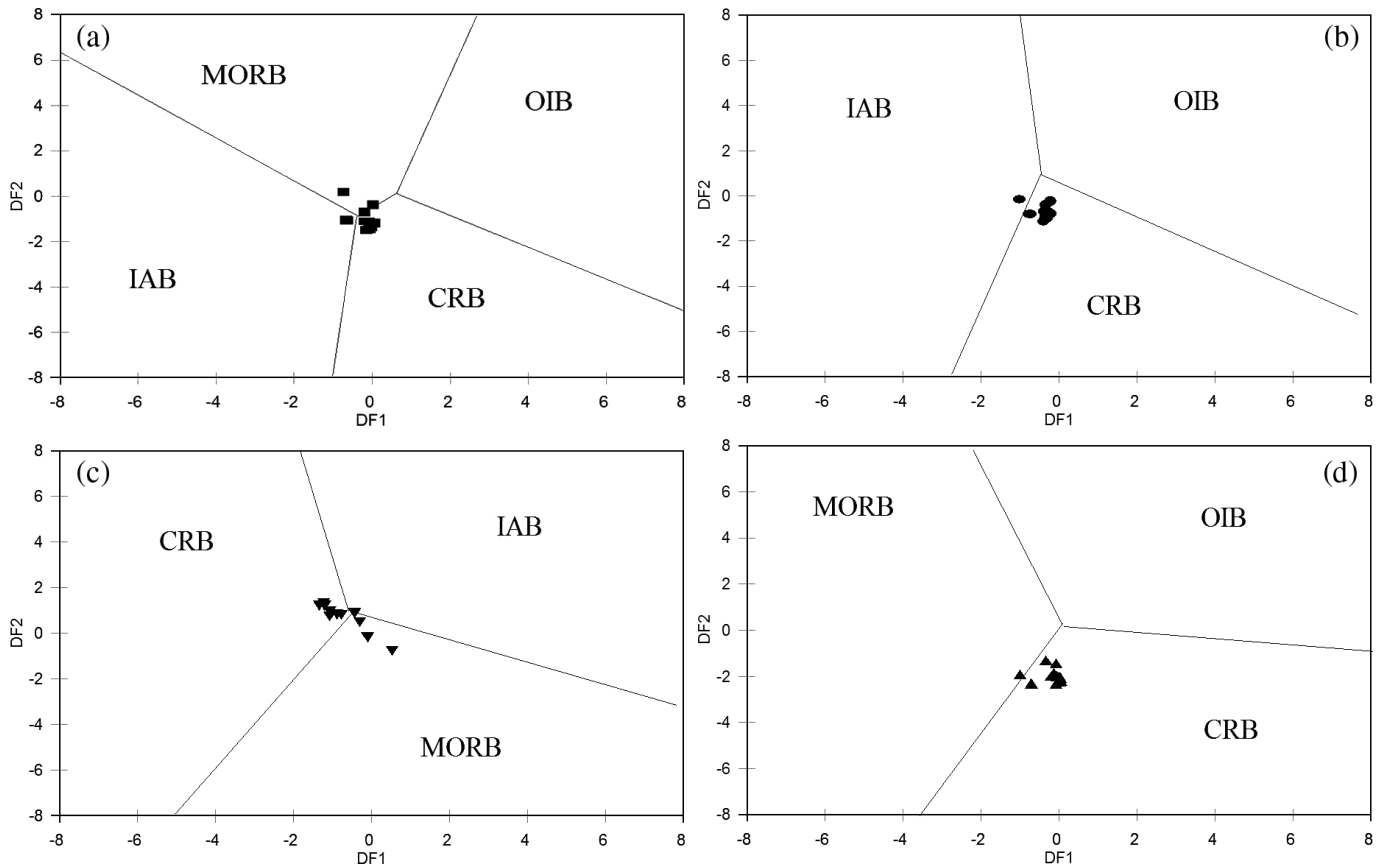
The Cerro Verde volcanic field is located ~45 km southwest of Albuquerque (Fig. 1). Flows fill the paleochannel of the ancestral Rio San Jose and cross the Rio Grande rift – Colorado Plateau boundary without any apparent offset. Flows have been dated at about 320 Ka (Leavy et al. 1987).

Mesita Negra volcanic field is located about 26 km west of Albuquerque (Fig. 1) and is composed of basaltic flows. A flow interbedded with the Ceja Formation of the Santa Fe Group has been dated at 8.11 ± 0.05 Ma (Maldonado et al. 1999) using the ⁴⁰Ar/³⁹Ar method.

Geochronology method and results

The whole-rock samples were crushed sieved, treated with dilute HCL, washed in distilled water and hand-picked to remove phenocrysts, weathered material, etc., leaving as pure a groundmass concentrate as possible. They were then placed in a machined Al disc and sealed in an evacuated Pyrex tube along with inter-laboratory standard Fish Canyon Tuff (age = 27.84 Ma). The standard was used to monitor the neutron dose received during the 1 h (NM-51) or 2 h (NM-61) irradiation in the D-3 position of the reactor at the Nuclear Science Center, College Station, Texas. The groundmass concentrate samples were step-heated in a double vacuum Mo resistance furnace. The gas was gettered during heating with a SAES GP-50 getter for 7 min, and additionally cleaned following heating with another GP-50 for an additional 5 min. The flux monitor crystals were placed in a copper planchet and fused within an ultra-high vacuum argon extraction system with a 10 W Synrad CO₂ continuous laser. Evolved gases were purified for 2 min using a SAES GP-50 getter operated at about 450 °C. Argon isotopic compositions for both the samples and monitors were determined with a MAP 215-50 mass spectrometer operated in electron

Fig. 8. (a) Discriminant diagram of island-arc basalt (IAB) – continental-rift basalt (CRB) – ocean-island basalt (OIB) – mid-oceanic ridge basalt (MORB) types (Agrawal et al. 2004) displaying samples from Cat Hills, Cat Mesa, Wind Mesa, Cerro Verde, and Mesita Negra. All of the samples plot in either the CRB or IAB fields with the exception of CH-11, which contains the lowest MgO content (2.6%) of all the samples in this study. (b) Discriminant diagram of IAB–CRB types (Agrawal et al. 2004) displaying samples from Cat Hills, Cat Mesa, Wind Mesa, Cerro Verde, and Mesita Negra. Sample CH-11 plots in the IAB field. (c) Discriminant diagram of IAB–CRB–MORB types (Agrawal et al. 2004) displaying samples from Cat Hills, Cat Mesa, Wind Mesa, Cerro Verde, and Mesita Negra.. Samples CH-10, CH-11, and WM-01A plot in the MORB field, although CH-10 and CH-11 have contrasting compositions. Sample CH-10 is high in MgO (8.34%) compared with sample CH-11 (2.60%). (d) Discriminant diagram of CRB–OIB–MORB types (Agrawal et al. 2004) displaying samples from Cat Hills, Cat Mesa, Wind Mesa, Cerro Verde, and Mesita Negra. Sample CH-11 plots in the MORB field. (a–d) DF1 and DF2 are discriminant factors 1 and 2, respectively.



multiplier mode with an overall sensitivity of 3.0×10^{-17} mol/pA. Extraction system and mass spectrometer blanks and backgrounds were measured numerous times throughout the course of the analyses. Typical blanks (including mass spectrometer backgrounds) were 570, 4, 0.3, 0.8 and 2.6×10^{-18} moles at masses 40, 39, 38, 37, and 36, respectively. J -factors were determined to a precision of 0.25% by analyzing four single crystal aliquots from each of the four radial positions around the irradiation vessel. Corrections for interfering nuclear reactions were determined using K-glass and CaF_2 . These values are $(^{40}\text{Ar}/^{39}\text{Ar})_{\text{K}} = 0.00020 \pm 0.0003$, $(^{36}\text{Ar}/^{37}\text{Ar})_{\text{Ca}} = 0.00026 \pm 0.00002$ and $(^{39}\text{Ar}/^{37}\text{Ar})_{\text{Ca}} = 0.00070 \pm 0.00005$. All errors are reported at the 2σ confidence level and the decay constant and isotopic abundance are those suggested by Steiger and Jager (1977).

The available age data from the study area and the location of the samples collected and analyzed are summarized in Table 1. Age spectra diagrams (Figs. 3–7) are given for five samples: CH-21 and CH-3 (Cat Hills), CM-01A (Cat Mesa),

WM-01A (Wind Mesa), and CH-11 (Mesita Negra). These groundmass concentrates yielded fairly well-behaved age spectra. A weighted mean age of 0.11 ± 0.03 Ma was calculated from 98.9% of the ^{39}Ar released from the Cat Hills sample (CH-21, Fig. 3a). Inverse isochron data from this sample yielded a $^{40}\text{Ar}/^{36}\text{Ar}$ intercept of 298.6 ± 4.8 that agreed within error to the atmospheric ratio (295.5) and an isochron age of 0.09 ± 0.03 Ma that was within error of the weighted mean age (Fig. 3b). CH-3 age spectra yielded old apparent ages in the early and late heating steps (Fig. 4a). A weighted mean age of 0.14 ± 0.03 Ma was calculated from the flattest mid-portion of the spectrum. Steps A–I were evaluated with the inverse isochron technique and revealed an isochron age of 0.09 ± 0.03 Ma with an $^{40}\text{Ar}/^{36}\text{Ar}$ intercept of 303.4 ± 2.1 (Fig. 4b). The age spectra from the Cat Mesa (CM-01A) basalt revealed old apparent ages in the early heating steps and young apparent ages in the late heating steps. A weighted mean age of 3.01 ± 0.12 Ma that contained 67.1% of the ^{39}Ar released was calculated from the

flattest mid-portion of the spectrum (Fig. 5a). Steps A–F were evaluated with the inverse isochron technique and yielded an isochron age of 2.99 ± 0.25 Ma and a $^{40}\text{Ar}/^{36}\text{Ar}$ intercept of 309 ± 5 (Fig. 5b). Although the $^{40}\text{Ar}/^{36}\text{Ar}$ intercept was slightly above the atmospheric ratio, we noted that the error on the isochron age was twice that of the weighted mean age calculated from the age spectrum. A weighted mean age of 4.15 ± 0.17 Ma was calculated from 96.6% of the ^{39}Ar released from the WM-01A groundmass concentrate (Fig. 6a). Inverse isochron analysis of steps A–L revealed an isochron age of 4.01 ± 0.16 Ma with a $^{40}\text{Ar}/^{36}\text{Ar}$ intercept of 299.4 ± 2.2 that was slightly above the atmospheric ratio (Fig. 6b). The Mesita Negra basalt also yielded a well-behaved spectra, and a weighted mean age of 8.11 ± 0.05 Ma was calculated from 84.9% of the ^{39}Ar released (Fig. 7a). Steps C–G yielded an isochron age of 8.13 ± 0.06 Ma with a $^{40}\text{Ar}/^{36}\text{Ar}$ intercept of 280 ± 42 that was within error of the atmospheric ratio (Fig. 7b). The weighted mean ages calculated from CH-21, CM-1, and CH-11 age spectra (0.11 ± 0.03 , 3.00 ± 0.10 , and 8.11 ± 0.05 Ma, respectively) were assigned as the eruption ages of the basalts. The inverse isochron age calculated from WM-01A (4.01 ± 0.16 Ma) was assigned as the eruption age of the Wind Mesa basalt because the $^{40}\text{Ar}/^{36}\text{Ar}$ intercept was slightly above the atmospheric ratio and the inverse isochron was well-behaved. We have also assigned the isochron age of CH-3 (0.09 ± 0.03 Ma) as the eruption age. We noted that this age agreed within error to the eruption age calculated for CH-21, which was collected from the same Cat Hills basalt flow.²

Geochemistry methods

The oxide abundances of 10 major and minor rock-forming elements (SiO_2 , TiO_2 , Al_2O_3 , total Fe as Fe_2O_3 , MgO , CaO , Na_2O , K_2O , P_2O_5 , MnO) of the rock samples were determined by wavelength-dispersive X-ray fluorescence (WD-XRF). To obtain loss on ignition (LOI), a 0.8 g portion of sample was ignited at 925 °C for 45 min. The sample was then fused with lithium borate flux to create a homogeneous pellet for analysis. The precision of the major and minor elemental determinations is typically better than 1%, based on replicate analysis of prepared standards, whereas accuracy is better than 2%. A full description of the WD-XRF technique is given in Taggart and Siems (2002).

The abundances of 33 major, minor and trace elements, including 11 rare-earth elements (REE's), were determined from the rock samples by instrumental neutron activation analysis (INAA). Samples of about 1 gm of each were irradiated in the USGS-TRIGA reactor at a flux of 2.5×10^{12} for 8 h. Three sequential counts at 7, 14, and 65 days after the irradiation were made on both coaxial and planar germanium detectors. A summary of the INAA procedure used at the USGS is given in Budahn and Wandless (2002). Precision and accuracy for most of the elements ranged from 1% to 5%, including La, Yb, Hf, Ta, Rb, Th, and U. Only five elements had precision errors of >10% (Ho, Tm, W, Sb and Au) based on counting statistic errors. Accuracy was based

on replicate analysis of USGS standard reference materials, including BHVO-1.

Isotopic analyses for $^{87}\text{Sr}/^{86}\text{Sr}$ and $^{143}\text{Nd}/^{144}\text{Nd}$ ratios and ratios of ^{206}Pb , ^{207}Pb , and ^{208}Pb versus ^{204}Pb were performed on the same powder splits analyzed by WD-XRF and INAA. Analytical procedures for Sr, Nd, and Pb analyses were similar to those reported by Stille et al. (1986). Samples were dissolved in PFA-Teflon screw-cap jars using nitric and hydrofluoric acids. Lead was separated using anion exchange chromatography in 1.0 mol/L HBr medium. Strontium and the REEs were separated using cation exchange chromatography in 0.2 mol/L 2-methylactic acid medium. Analytical blanks were $\text{Pb} = 0.3$ ng, $\text{Sr} = 0.5$ ng, and $\text{Nd} = 0.1$ ng. The analytical blanks for all three elements are insignificant relative to the amounts in the sample. Lead isotopic analyses were obtained using a VG Sector-54, seven-collector solid-source mass spectrometer. Raw data were corrected for mass fractionation of $0.13\% + 0.03\%$ per AMU (atomic mass unit) based on replicate analysis of National Institute of Standards (NIST) standard SRM 981 (values determined by Todt et al. 1993). Strontium and neodymium isotopic analyses were obtained using a Micromass 54R single-collector solid-source mass spectrometer. Ten analyses of NIST standard SRM 987 gave a mean $^{87}\text{Sr}/^{86}\text{Sr} = 0.710258 \pm 0.000008$ (95% confidence interval (CI); Ludwig 1994). Twelve analyses of the La Jolla Nd standard gave a mean $^{143}\text{Nd}/^{144}\text{Nd} = 0.511852 \pm 0.000008$ (95% CI).

Results and discussion

The geochemical and isotopic data on the 13 samples from the Cat Hills, Cat Mesa, Wind Mesa, Cerro Verde, and Mesita Negra volcanic centres are given in Tables 2–4. Major element compositions on rocks from this area have been reported previously by Kelley and Kudo (1978) and are given in Table 5. The eight samples from Cat Hills have moderately high (>6.4%) MgO and low (<50%) SiO_2 content and are similar in composition to some continental flood basalts (Table 3). The two samples from Cat Mesa and Wind Mesa appear to be slightly more evolved than the Cat Hills rocks with MgO abundances of about 5.5%. The Mesita Negra sample has the lowest MgO content (2.5%). Despite their low MgO content, these later four samples still have fairly low in SiO_2 contents (<52%) and high CaO (>8.15%), precluding a fractional-crystallization relationship involving clinopyroxene. A positive correlation between CaO – MgO contents is common in rocks with <7% MgO and is controlled by Ca-rich pyroxene (Cox 1980). All of the samples are olivine normative. The Mesita Negra rock is also nepheline normative.

According to the discriminant diagrams of Agrawal et al. (2004) that utilize hydrous-free major element data, these samples most often plot in CRB fields (Figs. 8a–8d) although a significant number of samples plot in the MORB field (Fig. 8c) (CRB–MORB–IAB (island-arc basalt)). This latter result might be expected given that MORB-like sources could be involved in producing CRB magmas. However, it is clear from the examination of the trace element and isotopic data

²Auxiliary information on the geochronology methods and results can be found at http://geoinfo.nmt.edu/publications/openfile/argon/27/NMBGMR_OF-AR-27.pdf.

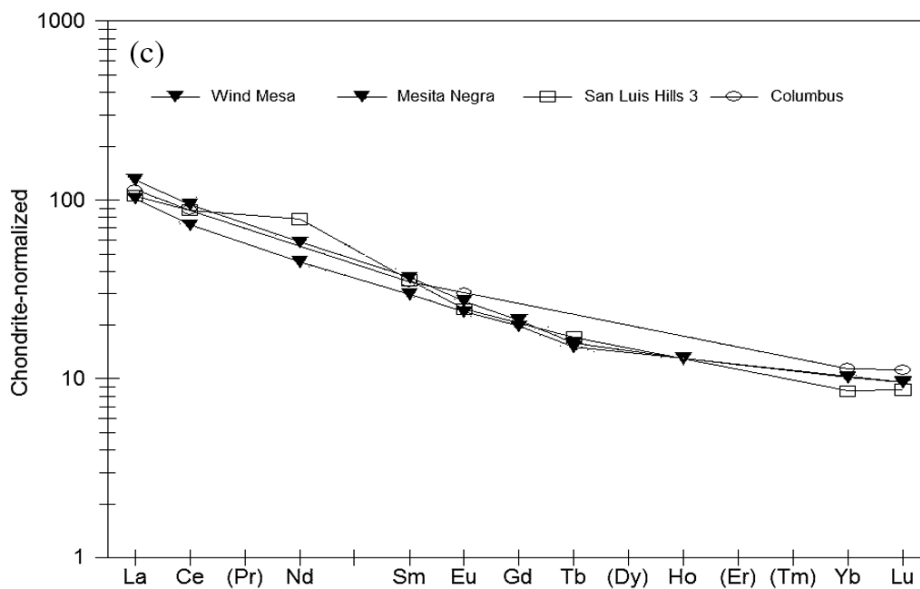
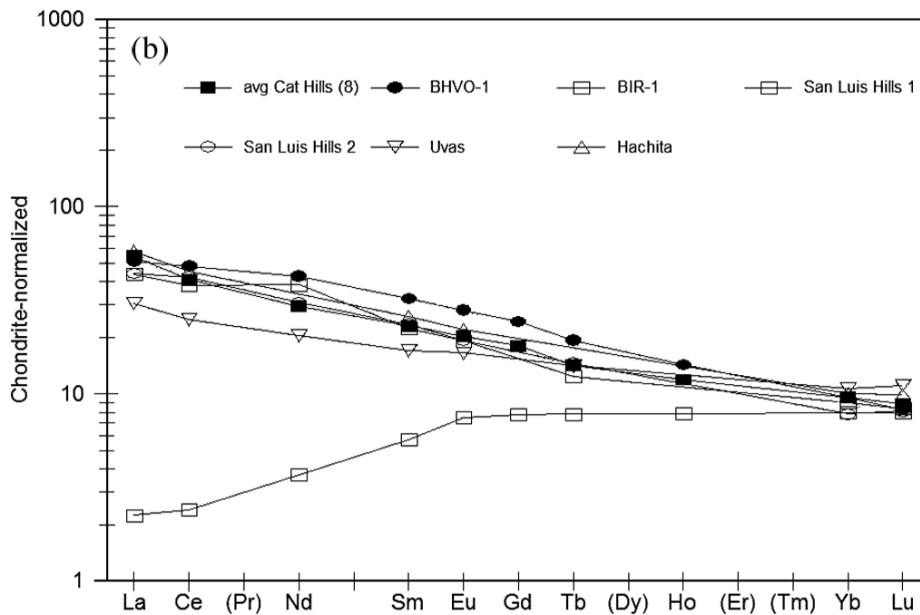
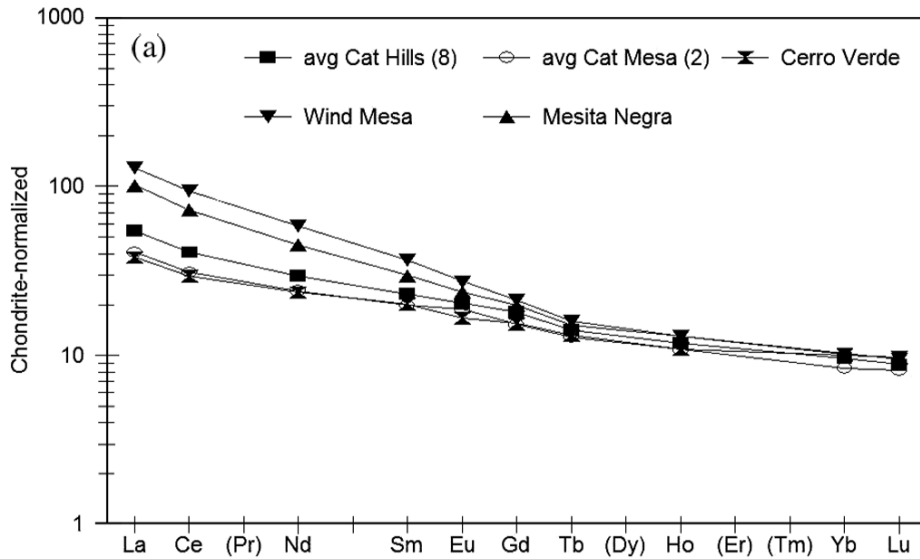


Fig. 9. (a) Chondrite-normalized rare-earth element (REE) abundance patterns of the Cat Hills, Cat Mesa, Cerro Verde, Wind Mesa, and Mesita Negra rocks of this study. REEs in parenthesis were not determined. The samples used to obtain the average Cat Hills REE composition are CH-1, CH-3, CH-5, CH-06A, CH-7, CH-8, CH-9, and CH-21. The Cat Mesa REE pattern is the average of samples CM-01A and CM-04. Chondrite normalization values are from Boynton (1985). (b) Average REE abundance pattern of the Cat Hills rocks compared with US Geological Survey standard reference materials BHVO-1 and BIR-1. Other Rio Grande rift lavas with similar REE patterns are also plotted (see text). BHVO-1 is representative of an ocean-island basalt (OIB) type, whereas BIR-1 has a REE pattern typical of mid-oceanic ridge basalt (MORB) type. The San Luis Hill and Uvas samples are early rift (>20 Ma) volcanic rocks. The Hatchita sample has been dated at 11.8 Ma (McMillan et al. 2000). Chondrite normalization values are from Boynton (1985). (c) REE abundance patterns of the Wind Mesa and Mesita Negra rocks are compared with other Rio Grande rift lavas with similar REE patterns (see text). The San Luis Hill sample is an early rift (>20 Ma) volcanic rock, whereas the Columbus sample has been dated at 3.0 Ma (McMillan et al. 2000). Chondrite normalization factors are from Boynton (1985).

that these samples are more similar to OIB type rocks than to MORB type rocks. In addition, (as was stated earlier in the text), McMillan et al. (2000) contends that younger Rio Grande rift rocks (<10 Ma) are dominantly derived from an asthenospheric mantle, which is the likely source of many OIB magmas (e.g., Hawaiian rocks). All of the rocks from this study are of this age (<8 Ma). If this is correct, then it could be argued that CRB compositions from some tectonic settings may actually be more representative of, or equivalent to, OIB rocks. In fact, an inspection of the Agrawal et al. (2004) data sets does show that there is considerable overlap between CRB and OIB major element compositions, especially on the IAB–CRB–OIB–MORB diagram.

With respect to the incompatible trace elements, the REE's, Rb, Sr, Cs, Zr, Hf, and Ta contents in the Cat Hills samples are remarkably similar to those found in some Hawaiian basalts (Table 4); in contrast, Ba, Th, and U are somewhat higher in these samples relative to Hawaiian rocks. These samples are also similar in composition to some Hawaiian rocks in the olivine-compatible elements, Cr, Ni and Co, but are lower in Sc. The Cat Mesa and Cerro Verde samples are generally poorer in incompatible trace elements compared with Cat Hills, whereas the Wind Mesa rock is significantly enriched with these elements. In most cases, the Mesita Negra sample is intermediate in incompatible trace element contents, and between the Cat Mesa and Wind Mesa samples in composition. The Cr, Ni, Co, and Sc contents of the Cat Hills and Wind Mesa samples are slightly lower than the Cat Hills samples, consistent with their lower MgO abundances; the Cerro Verde sample has the highest content of MgO (8.26%) and Ni (210 ppm). Differences in trace element contents among the samples are displayed in Fig. 9a where the abundances of the REE's are normalized to chondrites (Boynton 1985).

Rocks somewhat similar in major element and REE composition to the central New Mexico samples are found in other Rio Grande rift volcanic fields. For example, Fig. 9b presents the REE abundance patterns of two samples (San Luis Hills 1 and 2) as reported by Thompson et al. (1991) and two samples (Uvas and Hatchita) as reported by McMillan et al. (2000); these are comparable to the average Cat Hills flows. Also plotted in Fig. 9b are REE patterns of two USGS standard reference materials, BHVO-1 and BIR-1, which are considered representative of OIB type and MORB type rocks. The two San Luis Hills samples from Thompson et al. (1991) are the most mafic rocks (>6.9% MgO) from their suite 3 lavas. Johnson and Thompson (1991) conclude that these 26 Ma lavas have assimilated large amounts of crust. The two mafic rocks (Uvas and Hatchita) reported by

McMillan et al. (2000) were erupted 27 and 11.8 Ma ago, respectively, and contain 8.0% and 7.6% MgO. These magmas are also interpreted to be partial melts, contaminated with lower crust.

Plotted in Fig. 9c are REE patterns of the Wind Mesa and Mesita Negra samples. In general, most of the more mafic (>6.5%) Rio Grande rift samples reported by Thompson et al. (1991) and McMillan et al. (2000) have REE abundance similar to these rocks. The suite 1 San Luis Hills 3 sample (Thompson et al. 1991) contains 8.11% MgO and the Columbus, New Mexico sample (McMillan et al. 2000) contains 8.70% MgO and is typical of the LREE-enriched Oligocene Rio Grande rift lavas. According to Johnson and Thompson (1991), the suite 1 rocks have isotopic compositions that reflect minimal interaction with the crust.

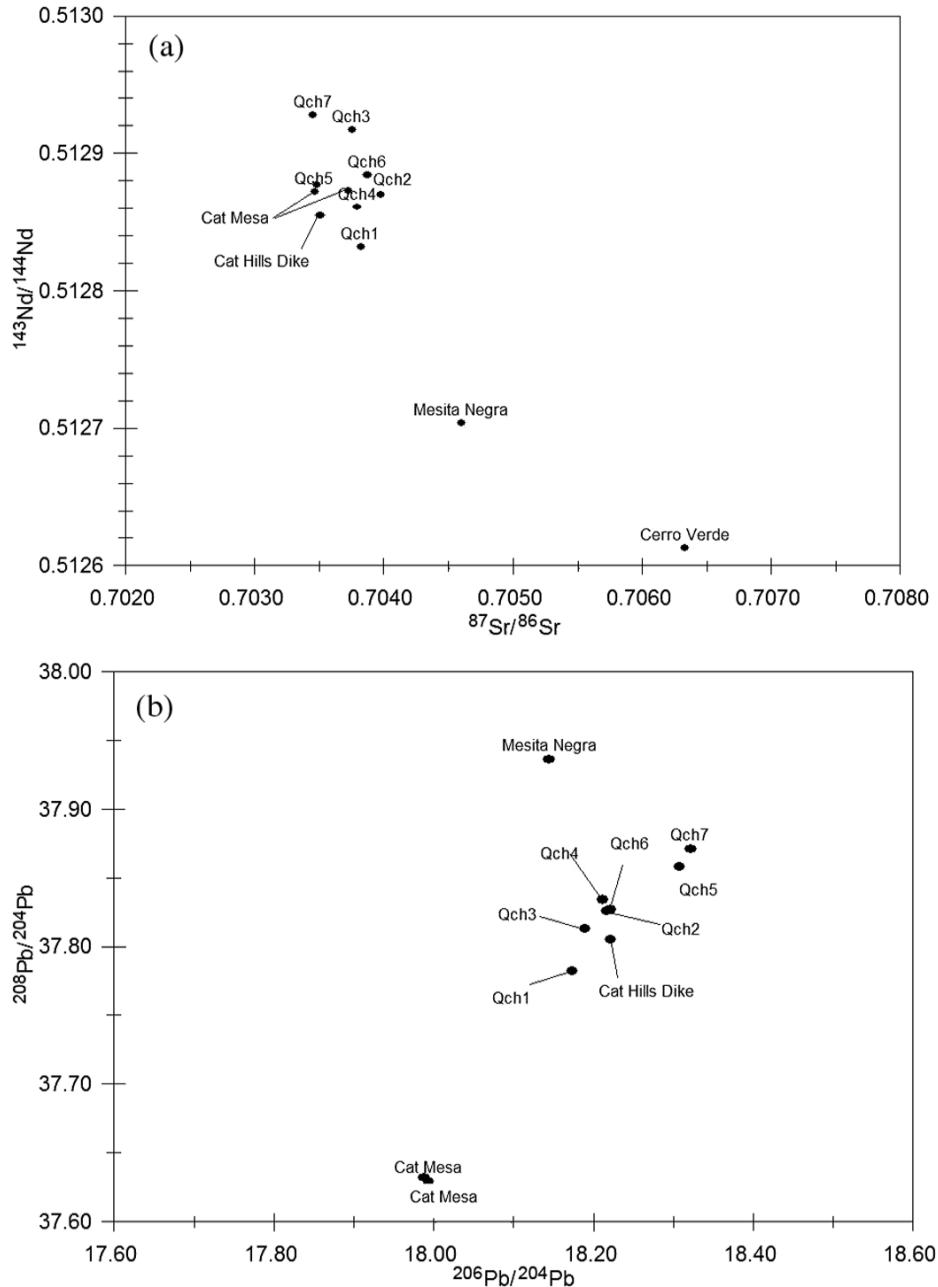
The Cat Hills and Cat Mesa samples have similar Sr and Nd isotopic compositions but different Pb signatures (Figs. 10a–10b). Two flows from Cat Hills also appear to have different Pb isotopic ratios compared with the other five flows and the dike. The Sr and Nd isotopes of the Cerro Verde and Mesita Negra samples are more radiogenic than Cat Hills and Cat Mesa rocks; although there are no Pb isotopic data for the Cerro Verde rock, the Mesita Negra sample clearly has a unique Pb signature. There are no Sr, Nd, and Pb isotopic data available for the Wind Mesa sample.

Despite the isotopic differences between the Cat Hills and Cat Mesa samples, Sr, Nd and Pb signatures from all of these rocks are either OIB-like or MORB-like. Although the Cerro Verde and Mesita Negra Sr and Nd values are more radiogenic (Fig. 11a) than the Cat Hills rocks, their Pb values also plot in the OIB–MORB field (Fig. 11b).

The six Rio Grande rift samples discussed earlier in the text from Johnson and Thompson (1991) and McMillan et al. (2000) are also plotted in Figs. 11a and 11b. The depleted mantle compositions plotted in these figures are the isotopic signatures of a depleted MORB type mantle proposed by Ito and Mahoney (2005). EM1 and EM2 are enriched mantles 1 and 2 and are also taken from Ito and Mahoney (2005). The upper crust (UC) and lower crust (LC) values plotted on Fig. 11b are from McMillan et al. (2000) study of Rio Grande rift magmatism.

With the exception of the Columbus sample, all of the Rio Grande rift rocks from these other studies plot outside the Nd–Sr OIB–MORB field on Fig. 7a, which is consistent with these authors' interpretation that the lavas contain significant crustal components. Most of their samples also plot outside the Pb OIB–MORB field on Fig. 7b. On this basis, we propose that lavas from the rift-related central

Fig. 10. (a) $^{143}\text{Nd}/^{144}\text{Nd}$ vs. $^{87}\text{Sr}/^{86}\text{Sr}$ isotopic ratios of the Cat Hills, Cat Mesa, Cerro Verde and Mesita Negra rocks. Seven of the Cat Hill samples are denoted with Qch prefixes and represent layered flows. (b) $^{208}\text{Pb}/^{204}\text{Pb}$ vs. $^{206}\text{Pb}/^{204}\text{Pb}$ isotopic ratios of the Cat Hills, Cat Mesa, and Mesita Negra rocks.

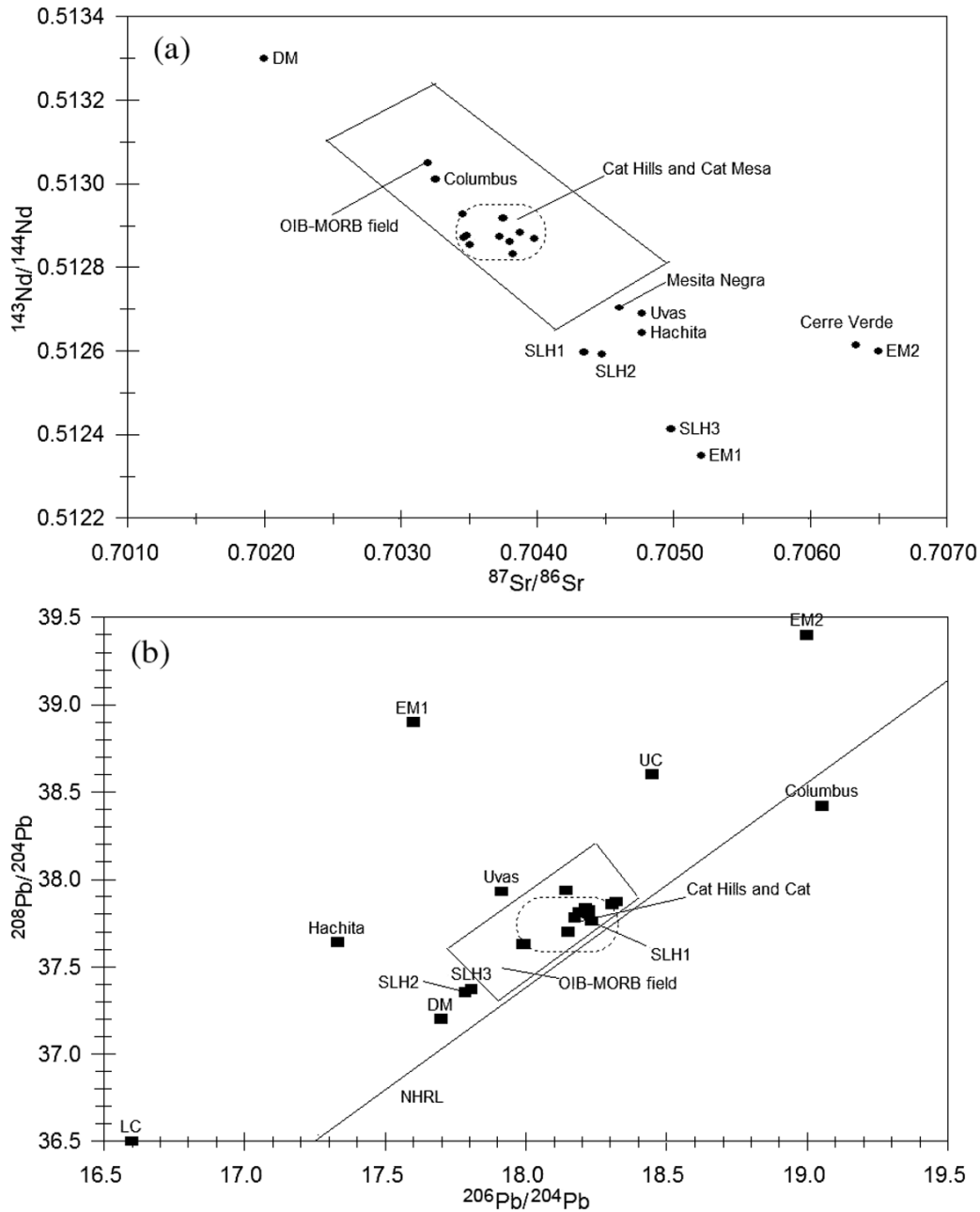


New Mexico volcanoes of this study were produced from the melting of an OIB-source and possibly a MORB-source, and that interaction with continental lithosphere or crust was minimal. One of these components may be similar to EM1 proposed by Ito and Mahoney (2005) (Figs. 7a–7b) to account for the composition of the Mesita Negra rock. A very small contribution of lower crustal material, however, may have affected the Pb values in the Cat Mesa rocks. Although no Pb data is available for the Cerro Verde sample, the Sr and Nd data suggest that this rock was generated from a dif-

ferent enriched mantle (EM2). A unique origin for this rock is consistent with the fact that this lava erupted adjacent to the Rio Grande rift in the Colorado Plateau.

Based on the similar whole rock composition and age of the Wind Mesa sample to the Cat Mesa samples, we interpret the enriched trace element composition of the Wind Mesa lava to be the result of a lower degree of partial melting of the Cat Mesa source. Isotopic data on this sample, however, could indicate the presence of additional mantle or crustal components.

Fig. 11. (a) $^{143}\text{Nd}/^{144}\text{Nd}$ vs. $^{87}\text{Sr}/^{86}\text{Sr}$ isotopic ratios of the Cat Hills, Cat Mesa, Cerro Verde, and Mesita Negra rocks. Isotopic signatures of a depleted mantle (DM), ocean-island basalt (OIB) – mid-oceanic ridge basalt (MORB) type field, enriched mantle 1 (EM1), and enriched mantle 2 (EM2) are shown for comparison (see text). Also plotted are six samples from other Rio Grande rift eruptions. It is noted that the younger rocks, i.e., Columbus (3.0 Ma), Cat Hills (<140 Ka), and Cat Mesa (3.0 Ma) plot within the OIB–MORB field whereas the older rocks, i.e., Mesita Negra (8.11 Ma) and Hachita (11.8 Ma), plot outside this field. The San Luis Hill samples (SLH prefixes) have been interpreted to be derived from distinct sources and are > 20 Ma (Johnson and Thompson 1991). The Uvas sample is 27 Ma. The Cerro Verde sample has not been dated. (b) $^{208}\text{Pb}/^{204}\text{Pb}$ vs. $^{206}\text{Pb}/^{204}\text{Pb}$ isotopic ratios of the Cat Hills, Cat Mesa and Mesita Negra rocks. Isotopic signatures of a DM, OIB–MORB type field, EM1, EM2, lower crust (LC), upper crust (UC), northern hemisphere reference line (NHRL), and six Rio Grande rift lavas from other eruptions are shown for comparison (see text). Although there is considerable overlap of Pb compositions with respect to age, the younger (<10 Ma) Rio Grande rift samples tend to have higher $^{208}\text{Pb}/^{204}\text{Pb}$ and $^{206}\text{Pb}/^{204}\text{Pb}$ values than older (>20 Ma) samples (McMillan et al. 2000).



Conclusions

Differences in ages, geochemistry and isotopic composition suggest that basaltic flows, erupted from each of the volcanic centres of Cat Hills, Cat Mesa, Wind Mesa, Cerro Verde, and Mesita Negra, have unique origins.

The geochemical and isotopic compositions of the rocks from the volcanic fields of central New Mexico supports the conclusions of others (McMillan et al. 2000) that late Cenozoic Rio Grande rift basalts record a shift in the mantle region from lithosphere to upwelling asthenosphere. The oldest lavas from this area exhibit enrichments in trace element content, and differences in isotopic ratios, consistent with the involvement of either an enriched mantle or crustal component. The youngest rocks are very similar in composition to magmas generated from an OIB-source (e.g., Hawaiian rocks), which is generally thought to be the asthenosphere. This indicates that Rio Grande rifting has significantly thinned the lithosphere beneath the Cat Hills volcanic field.

Acknowledgments

This study was funded by the USGS National Cooperative Geologic Mapping Program as part of the Middle Rio Grande project. The authors thank Ren Thompson and Rick Page of the USGS for their review comments. Reviews by Surendra P. Verma and B. Edwards greatly improved the manuscript. Surendra P. Verma provided the CIPW calculations (personal communication, 2005). We also thank the people of Isleta, New Mexico.

References

- Agrawal, S., Guevara, M., and Verma, S.P. 2004. Discriminant analysis applied to establish major-element boundaries for tectonic varieties of basic rocks. *International Geology Review*, **46**: 575–594.
- Boynton, W.V. 1985. Geochemistry of the rare earth elements: meteorite studies. *In* Developments in geochemistry 2, rare earth element geochemistry. *Edited by* P. Henderson. Elsevier, Amsterdam, The Netherlands, pp. 115–152.
- Budahn, J.R., and Wandless, G.A. 2002. Instrumental neutron activation analysis by long count. Chapter X. *In* Analytical methods for chemical analysis of geologic and other materials. *Edited by* Joseph E. Taggart, Jr. US Geological Survey, Open File Report 02-0223, pp. X1–X13.
- Cox, K.G. 1980. A model for flood basalt volcanism. *Journal of Petrology*, **21**: 629–650.
- Ito, G., and Mahoney, J.J. 2005. Flow and melting of a heterogeneous mantle: 1. Method and importance to the geochemistry of ocean island and mid-ocean ridge basalts. *Earth and Planetary Science Letters*, **230**: 29–46.
- Johnson, C.M., and Thompson, R.A. 1991. Isotopic composition of Oligocene mafic volcanic rocks in the northern Rio Grande rift: evidence for contributions of ancient intraplate and subduction magmatism to evolution of the lithosphere. *Journal of Geophysical Research*. **96**: B8, 13 593 – 13 608.
- Kelley, V.C., and Kudo, A.M. 1978. Volcanics and related basaltic rocks of the Albuquerque–Belen Basin, New Mexico. New Mexico Bureau of Mines and Mineral Resources, Circular 156.
- Kudo, A.M., Kelley, V.C., Damon, P.E., and Shafiquallah, M. 1977. K–Ar ages of basalt flows at Canjilon Hill, Isleta volcano, and Cat Hills volcanic field, Albuquerque–Belen Basin, central New Mexico. *Isochron/West*, **18**: 15–16.
- Leavy B.D., Phillips, F.M., Elmore, D., Kubick, P.W., and Gladney, E. 1987. Measurement of cosmogenic $^{36}\text{Cl}/\text{Cl}$ in young volcanic rocks: an application of accelerator mass spectrometry in geochronology. *Nuclear Instruments and Methods in Physics Research*, **B26**: 246–250.
- Ludwig, K.R. 1994. Isoplot: a plotting and regression program for radiogenic-isotope data. US Geological Survey, Open-File Report 91-445, version 2.75.
- Maldonado, F. 2003. Geologic map of the Rio Puerco 7.5-minute Quadrangle, Valencia County, New Mexico. US Geological Survey, Miscellaneous Field Studies Map MF-2397, scale 1 : 24 000.
- Maldonado, F., and Atencio, A. 1998a. Preliminary geologic map of the Wind Mesa 7.5-minute Quadrangle, Bernalillo County, New Mexico. US Geological Survey, Open-File Report 97-740, scale 1 : 24 000.
- Maldonado, F., and Atencio, A. 1998b. Preliminary geologic map of the Dalies NW Quadrangle, Bernalillo County, New Mexico. US Geological Survey, Open-File Report 97-741, scale 1 : 24 000.
- Maldonado, F., Connell, S.D., Love, D.W., Grauch, V.J.S., Slate, J.L., McIntosh, W.C. et al. 1999. Neogene geology of the Isleta Reservation and vicinity, Albuquerque basin, central New Mexico. *In* New Mexico Geological Society, Guidebook 50, pp. 175–188.
- McMillan, N.J., Dickin, A.P., and Haag, D. 2000. Evolution of magma source regions in the Rio Grande rift, southern New Mexico. *Geological Society of America Bulletin*, **112**: 1582–1593.
- Okamura, S., Arculus, R.J., and Martynov, Y.A. 2005. Cenozoic magmatism of the north-eastern Eurasia margin: the role of lithosphere versus asthenosphere. *Journal of Petrology*, **46**: 221–253.
- Steiger, R.H., and Jager, E. 1977. Subcommittee on geochronology: convention on the use of decay constants in geo- and cosmochronology. *Earth and Planetary Science Letters*, **36**: 359–362.
- Stille, P., Unruh, D.M., and Tatsamoto, M. 1986. Pb, Sr, Nd and Hf isotopic constraints on the origin of Hawaiian basalts and evidence for a unique mantle source. *Geochimica et Cosmochimica Acta*, **50**: 2303–2319.
- Taggart, J.E., Jr., and Siems, D.F. 2002. Major element analysis by wavelength dispersive X-ray fluorescence spectrometry. Chapter T. *In* Analytical methods for chemical analysis of geologic and other materials. *Edited by* Joseph E. Taggart, Jr. US Geological Survey, Open File Report 02-0223, T1–T9.
- Thompson, R.A., Johnson, C.M., and Mehnert, H.H. 1991. Oligocene basaltic volcanism of the northern Rio Grande rift: San Luis Hills, Colorado. *Journal of Geophysical Research*, **96** (B8): 13 577–13 592.
- Todt, W., Cliff, R.A., Hanser, A., and Hofmann, A.W. 1993. Re-calibration of NBS lead standards using a ^{202}Pb – ^{205}Pb double spike. 7th annual meeting of the European Union of Geosciences, 4–8 April 1993, Strasbourg, France. Abstract, p. 396.
- Velasco-Tapia, F., Guevara, M., and Verma, S.P. 2001. Evaluation of concentration data in geochemical reference samples. *Chemie der Erde*, **64**: 69–91.